

## Universality and Scaling in Gravitational Collapse of a Massless Scalar Field

Matthew W. Choptuik

*Center for Relativity, University of Texas at Austin, Austin, Texas 78712-1081*

(Received 22 September 1992)

I summarize results from a numerical study of spherically symmetric collapse of a massless scalar field. I consider families of solutions,  $\mathcal{S}[p]$ , with the property that a critical parameter value,  $p^*$ , separates solutions containing black holes from those which do not. I present evidence in support of conjectures that (1) the strong-field evolution in the  $p \rightarrow p^*$  limit is universal and generates structure on arbitrarily small spatiotemporal scales and (2) the masses of black holes which form satisfy a power law  $M_{\text{BH}} \propto |p - p^*|^\gamma$ , where  $\gamma \approx 0.37$  is a universal exponent.

PACS numbers: 04.20.Jb

The model problem [1–5] of a single, massless scalar field,  $\phi$ , minimally coupled to the gravitational field,  $g_{\mu\nu}$ , provides one of the simplest arenas in which to investigate the nature and consequences of nonlinearity in general relativity [6]. With large-scale computation and advanced numerical techniques, it is now possible to make detailed surveys of the phenomenology of the model. Here I summarize such a survey which reveals several intriguing nonlinear phenomena arising in the regime where black holes form, or “almost form.”

The general time-dependent, spherically symmetric metric can be written

$$ds^2 = -\alpha^2(r, t) dt^2 + a^2(r, t) dr^2 + r^2 d\Omega^2, \quad (1)$$

where the radial coordinate  $r$ , which directly measures proper surface area, is a geometric quantity. A geometric time variable is provided by the proper time of a central observer,

$$T_0 \equiv \int_0^t \alpha(0, \tilde{t}) d\tilde{t}. \quad (2)$$

Introducing the auxiliary scalar field variables  $\Phi \equiv \dot{\phi}$  and  $\Pi \equiv a\dot{\phi}/\alpha$ , where an overdot denotes  $\partial/\partial t$  and a prime denotes  $\partial/\partial r$ , a sufficient set of equations for the model is

$$\dot{\Phi} = \left(\frac{\alpha}{a}\Pi\right)', \quad \dot{\Pi} = \frac{1}{r^2} \left(r^2 \frac{\alpha}{a}\Phi\right)', \quad (3)$$

$$\frac{\alpha'}{\alpha} - \frac{a'}{a} + \frac{1 - a^2}{r} = 0, \quad (4)$$

$$\frac{a'}{a} + \frac{a^2 - 1}{2r} - 2\pi r (\Pi^2 + \Phi^2) = 0. \quad (5)$$

The above system is invariant under the trivial rescaling  $r \rightarrow kr$ ,  $t \rightarrow kt$ , where  $k$  is an arbitrary positive constant—such transformations amount to a choice of units, and reflect the absence of a mass/length scale in the model. I will discuss the dynamics of the scalar field in terms of variables,  $X$  and  $Y$ , which are form-invariant under these transformations:

$$X(r, t) \equiv \sqrt{2\pi} \frac{r}{a} \Phi = \sqrt{2\pi} \frac{r}{a} \frac{\partial \phi}{\partial r}, \quad (6)$$

$$Y(r, t) \equiv \sqrt{2\pi} \frac{r}{a} \Pi = \sqrt{2\pi} \frac{r}{a} \frac{\partial \phi}{\partial t}. \quad (7)$$

In terms of these new variables, the total (conserved) mass,  $M$ , of the spacetime is

$$M = \int_0^\infty \frac{dm}{dr} dr = \int_0^\infty X^2 + Y^2 dr, \quad (8)$$

where the mass aspect function  $m$  is related to the metric function  $a$  in (1) by  $a^2 = (1 - 2m/r)^{-1}$ .

I solve Eqs. (3)–(5) using finite-difference techniques and an adaptive mesh-refinement algorithm [4, 7], where the basic scale of discretization,  $h$ , is allowed to vary locally (in both space and time) in response to the development of solution features. This adaptivity has been instrumental in the discovery and study of the phenomena described here which can unfold on arbitrarily small spatiotemporal scales. The large dynamic range required to resolve the phenomena and the extreme sensitivity of the solutions to initial conditions complicate the task of ensuring that the numerics faithfully represent the underlying physics. I have carefully examined this issue and will discuss it in detail elsewhere; here I assert that there is very strong evidence that the observed phenomena are *not* numerical artifacts.

Let  $\mathcal{S}$  denote a solution of (3)–(5). I have focussed study on one-parameter families of solutions,  $\mathcal{S}[p]$ , which are generated by evolving initially in-going packets (shells) of scalar field. Each family has the property that the parameter,  $p$ , characterizes the strength of the ensuing gravitational self-interaction of the scalar field. For each family, there is a parameter value,  $p_{\text{weak}}$ , such that in the limit  $p \rightarrow p_{\text{weak}}$ , the spacetime is flat and the evolution of the scalar field is described by a solution of the (linear) wave equation where the scalar wave packet implodes through  $r = 0$  and then escapes to infinity. At the other extreme is a parameter value,  $p_{\text{strong}}$ , such that as  $p \rightarrow p_{\text{strong}}$ , the end state of the evolution is a black hole formed by the collapse of the packet, with an arbitrarily small fraction of the scalar field escaping to infinity. Generically, between these two extremes is a “critical” parameter value,  $p^*$ , where black hole formation first occurs. Assuming that  $p_{\text{weak}} < p^* < p_{\text{strong}}$ , I will refer to solutions  $\mathcal{S}[p < p^*]$  and  $\mathcal{S}[p > p^*]$  as subcritical and supercritical, respectively. In both regimes, and for all the families I have considered, I have found that

the quantity  $\ln|p - p^*|$  is a natural choice for discussing the phenomenology of the solutions  $\mathcal{S}[p]$ .

From numerical studies of many families  $\mathcal{S}[p]$ , I have found two key features of strong-field ( $2m/r \approx 1$ ), near-critical dynamics as  $p \rightarrow p^*$ , which I formulate here as two conjectures. First, the precisely critical ( $p = p^*$ ) dynamical behavior is *universal*. In terms of the scalar field variables  $Z \equiv [X, Y]$ , there is a *unique* sequence,  $Z^*$ , which is naturally expressed as a function of logarithmic independent variables,  $\rho$  and  $\tau$ :

$$\rho \equiv \ln(kr) = \ln r + \kappa, \quad (9)$$

$$\tau \equiv \ln[k(T_0^* - T_0)] = \ln(T_0^* - T_0) + \kappa, \quad (10)$$

where the family-dependent constant  $\kappa = \ln k$  is chosen to normalize the overall scale (units) of the solution, and the constant  $T_0^*$  will be defined shortly. Second, the critical sequence,  $Z^*(\rho, \tau)$  satisfies a remarkable scaling relation:

$$Z^*(\rho - \Delta, \tau - \Delta) \simeq Z^*(\rho, \tau), \quad (11)$$

where  $\Delta$  is a *universal* constant with a numerical value of about 3.4. In order to understand the second conjecture from a physical viewpoint, it is important to emphasize that it pertains only to the *strong-field* dynamics of critical evolution, which always occurs in a neighborhood of  $r = 0$ . The scaling relation means that if I freeze a critical evolution at some time during the strong-field interaction and examine the profiles of  $X$  and  $Y$  out to some [imprecisely defined, hence the  $\simeq$  in (11)] maximum radius  $r_{\max}$ , then continue the evolution for a certain amount of geometric time  $\delta T_0$  and reexamine the solution on a scale  $e^\Delta \approx 30$  times smaller than previously, I will see the same field profiles. If I then wait an additional time interval  $\delta T_0/e^\Delta$  and “zoom in” by another factor of  $e^\Delta$ , I will again see the same profiles. Thus, a precisely critical configuration will be characterized by an infinite series of “echoes” in the field profiles (as well as any other form-invariant quantity such as  $a$ ,  $m/r$ , or  $dm/dr$ ), which arise from dynamics unfolding on increasingly smaller spatiotemporal scales. Because of the geometric relationship between the scales of suc-

TABLE I. Initial data specification for various one-parameter families discussed in text. For families (a)–(c), I specified the initial pulses to be purely in-going. For family (d), the functions  $X_>(r)$ ,  $Y_<(r)$  and  $X_<(r)$ ,  $Y_>(r)$  are late-time fits to subcritical and supercritical evolutions, respectively, of the pulse shape shown in Fig. 1(d).

Family	Form of initial data	$p$
(a)	$\phi(r) = \phi_0 r^3 \exp(-[(r - r_0)/\delta]^q)$	$\phi_0, r_0, \delta, q$
(b)	$\phi(r) = \phi_0 \tanh[(r - r_0)/\delta]$	$\phi_0$
(c)	$\phi(r + r_0) = \phi_0 r^{-5} [\exp(1/r) - 1]^{-1}$	$\phi_0$
(d)	$X(r) = (1 - \eta)X_<(r) + \eta X_>(r)$ $Y(r) = (1 - \eta)Y_<(r) + \eta Y_>(r)$	$\eta$

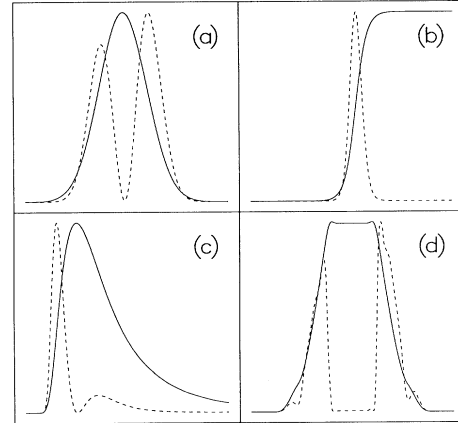


FIG. 1. Typical initial profiles of the scalar field  $\phi$  (solid lines) and the radial mass-energy density  $dm/dr$  (dotted lines) for the four families defined in Table I.

cessive echoes, the strong-field, critical evolution will conclude at some *finite* central proper time,  $T_0^*$ .

The numerical results I now summarize come from a study of several families of solutions characterized by the parametrized initial scalar field profiles listed in Table I. Representative initial profiles of  $\phi$  and  $dm/dr$  are shown in Fig. 1. For each family, I found a critical parameter value (to the limit of machine precision,  $\delta p/p \approx 10^{-13}$ ) using a binary search predicated on whether or a not a black hole formed during a calculation. Black hole formation is signaled by  $2m/r \rightarrow 1$  for some  $r_{\text{BH}}$ , from which the mass of the hole,  $M_{\text{BH}} = 2r_{\text{BH}}$ , immediately follows.

Figure 2 shows two profiles of the scalar field variable  $X$  from a *single* near-critical evolution of family (a) data. The curve marked with solid circles represents the

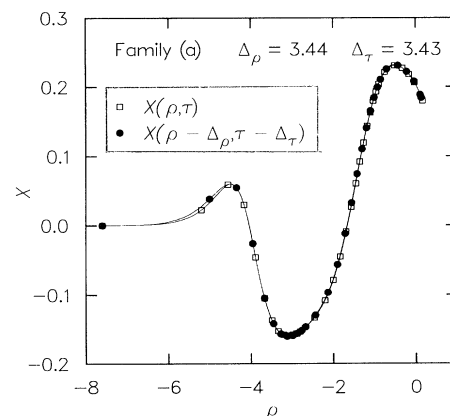


FIG. 2. Illustration of the rescaling or echoing property observed in near-critical evolution of the scalar field. The curve marked with open squares shows the profile of the scalar field variable,  $X$ , at some proper central time  $T_0$ . The curve marked with solid circles is the profile at a later time  $T_0 + e^{\Delta\tau}$  but on a scale  $e^{\Delta\rho} \approx 30$  times smaller.

“echo” of the earlier profile marked by squares. I determined the (radial) rescaling factor  $\Delta_\rho$  quoted in the figure by minimizing the total relative deviation between the early profile  $X(r, T_0)$  and the rescaled echo profile  $X(e^{\Delta_\rho r}, T_0 + e^{\Delta_\rho \tau})$ . I *independently* computed the temporal rescaling factor  $\Delta_\tau$  by estimating the critical time,  $T_0^*$ , for the calculation and then using the defining relation (10). The near equality of  $\Delta_\rho \approx 3.44$  and  $\Delta_\tau \approx 3.43$  provides additional evidence for conjecture (11).

Evidence for the *universality* of the strong-field evolution of a critical configuration is shown in Fig. 3 which displays profiles from near-critical evolutions for the families listed in Table I. Each group of four closely spaced lines consists of one profile from each family at a particular instant. Logarithmic time proceeds toward the back of the plot and the graph shows 3/4 of one cycle of the evolution. For each family, I chose a *single* value of  $\kappa$  to minimize the deviations among the profiles at the first time instant (front of the plot). This choice fixes the definitions of  $\rho$  and  $\tau$  for the subsequent instants. The close similarity of the profiles illustrates the uniqueness of the critical evolution, independent of the initial profile.

The results shown in Figs. 2 and 3 are all generated from the evolution of *subcritical* initial data sets. The critical regime may also be studied using *supercritical* evolutions which are characterized by the formation of black holes. In this case, in addition to the echoing be-

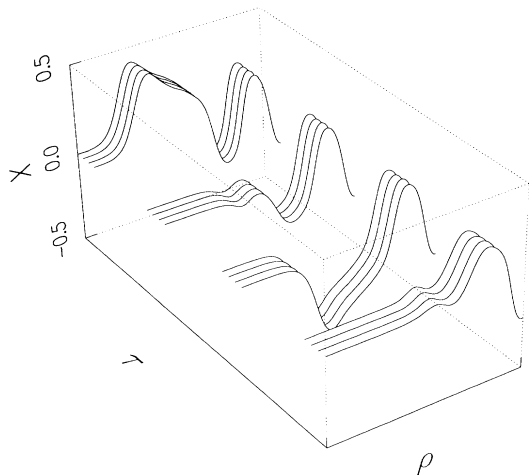


FIG. 3. Illustration of the conjectured universality of critical evolution in the model problem. Each group of four lines consists of one profile, at a particular instant,  $\tau$ , from near-critical evolution of each of the families listed in Table I [families (a)–(d), front to back]. For each family, I chose a single overall scaling constant,  $k$ , to maximize agreement among the first (foreground) group of curves. Agreement of the profiles at later times (towards the back of the plot) demonstrates universality of the evolution, regardless of initial pulse shape. Since these plots show less than one full cycle of evolution, echoing is not apparent here.

TABLE II. Numerically determined values of the scaling exponent  $\gamma$  in the conjectured relationship  $M_{\text{BH}} \simeq c_f |p - p^*|^\gamma$ .  $\mu_{\text{min}}$  and  $\mu_{\text{max}}$  are the minimum and maximum mass fractions ( $\mu \equiv M_{\text{BH}}/M$ ) of the black holes computed in the simulation and  $\gamma$  is the least-squares estimate of the scaling exponent.

Family	Parameter	$\mu_{\text{min}}$	$\mu_{\text{max}}$	$\gamma$
(a)	$\phi_0$	$7.9 \times 10^{-3}$	$8.9 \times 10^{-1}$	0.376
(a)	$\delta$	$1.3 \times 10^{-3}$	$9.4 \times 10^{-1}$	0.372
(a)	$q$	$3.1 \times 10^{-3}$	$9.8 \times 10^{-1}$	0.372
(a)	$r_0$	$1.3 \times 10^{-2}$	$9.2 \times 10^{-1}$	0.379
(b)	$\phi_0$	$2.8 \times 10^{-3}$	$4.0 \times 10^{-1}$	0.372
(c)	$\phi_0$	$4.9 \times 10^{-3}$	$9.9 \times 10^{-1}$	0.366
(d)	$\eta$	$2.2 \times 10^{-5}$	$1.7 \times 10^{-2}$	0.380

havior described above, I have observed another intriguing phenomenon. Empirically, the black hole mass is remarkably well described by a power law

$$M_{\text{BH}} \simeq c_f |p - p^*|^\gamma, \quad (12)$$

where  $c_f$  is a family-dependent constant, but where  $\gamma$  is an apparently *universal* scaling exponent which has a numerical value  $\gamma \approx 0.37$ . As Kaiser pointed out [8], this is suspiciously close to  $1/e = 0.367\dots$ . However, at this time I have no way of reliably assessing whether or not this is merely a numerical coincidence, nor do I know of any theoretical argument which would suggest that the critical exponent *should* have a value of  $1/e$ . Table II lists values of the exponent  $\gamma$  determined from least-squares fits to data generated from each of the four families. Also listed are the computed minimum and maximum mass fractions,  $\mu_{\text{min}}$  and  $\mu_{\text{max}}$ , of the black holes in each data set ( $\mu \equiv M_{\text{BH}}/M$ ). It is notable that in many cases the scaling law holds even for  $\mu$  close to unity, where almost all of the scalar field ends up in the black hole. Figure 4 plots the three data sets corresponding to the first three lines of Table II. The resulting near coincidence of the three sets of data points, as well as the near linearity of each set, is striking. Finally, I note that the mass-scaling relation (12) together with relation (11) strongly suggests that black hole formation generically turns on at *infinitesimal* mass in this model, rather than at a finite mass, as earlier calculations suggested [2].

The results described here provide a picture of the strong-field dynamics of a model problem which is in many ways considerably simpler than might have been anticipated. For near-critical configurations, it appears that virtually any “detail” that might appear in the specification of the initial data is “washed out” by the interaction between the scalar and gravitational fields. At the same time, the appearance of dimensionless quantities such as  $\Delta$  and  $\gamma$  is very interesting and has yet to be explained theoretically. It might be suspected that the simplicity and high degree of symmetry in the model are largely responsible for the observed behavior. However, extension of this work to a nonminimally coupled field [5]

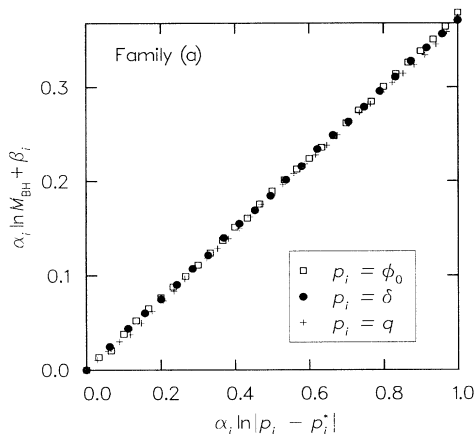


FIG. 4. Illustration of the conjectured mass-scaling relation (12). Data from three separate one-parameter variations of the pulse shape shown in Fig. 1(a) are shown. For each variation, I chose constants  $\alpha_i$  and  $\beta_i$  to normalize the ranges of the abscissa and place the data point corresponding to the smallest black hole in each family at the origin. The maximum ordinate value is  $1/e$ .

as well as investigations of the collapse of gravitational waves in axisymmetry [9] suggest phenomena of this type may occur generically in the strong-field interaction of massless fields and gravity.

I am grateful to J. R. Bond, D. Christodolou, N. Kaiser, R. Matzner, J. Thornburg, B. Unruh, and J. Winicour for discussions and encouragement. The re-

search was supported by the Natural Sciences and Engineering Research Council of Canada, by NSF Grant No. PHY-8806567, and by Texas Advanced Research Project Grant No. TARP-085. All numerical computations described here were performed at the Center for High Performance Computing, University of Texas System with Cray time supported by a Cray University Research grant to Richard Matzner.

- 
- [1] D. Christodolou, *Commun. Math. Phys.* **105**, 337 (1986); **106**, 587 (1986); **109**, 591 (1987); **109**, 613 (1987).
  - [2] D. Goldwirth and T. Piran, *Phys. Rev. D* **36**, 3575 (1987).
  - [3] R. Gómez, J. Winicour, and R. A. Isaacson, *J. Comput. Phys.* **98**, 11 (1992); R. Gómez and J. Winicour, *J. Math. Phys.* **33**, 1445 (1992); in *Approaches to Numerical Relativity*, edited by R. d'Inverno (Cambridge Univ. Press, Cambridge, 1992).
  - [4] M. W. Choptuik, in *Frontiers in Numerical Relativity*, edited by C. R. Evans, L. S. Finn, and D. W. Hobill (Cambridge Univ. Press, London, 1989).
  - [5] M. W. Choptuik, in *Approaches to Numerical Relativity* (Ref. [3]).
  - [6] K. S. Thorne, in *Nonlinear Phenomena in Physics*, edited by F. Claro (Springer-Verlag, Berlin, 1985).
  - [7] M. J. Berger and J. Olinger, *J. Comput. Phys.* **53**, 484 (1984).
  - [8] Nick Kaiser (private communication).
  - [9] A. M. Abrahams and C. R. Evans (private communication).